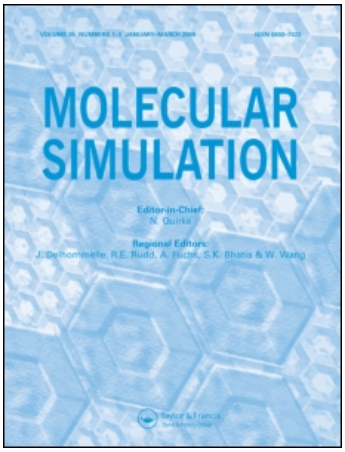

Molecular Simulation
Publication details, including instructions for authors and subscription information:
http://www.informaworld.com/smpp/title~content=t713644482

Applications of the ArgusLab4/AScore protocol in the structure-based binding affinity prediction of various inhibitors of group-1 and group-2 influenza virus neuraminidases (NAs)

Marija L. Mihajlovic[ab]; Petar M. Mitrasinovic[b]
[a] Department of Physical Chemistry, University of Belgrade, Belgrade, Serbia [b] Institute for Multidisciplinary Research, Belgrade, Serbia

To cite this Article Mihajlovic, Marija L. and Mitrasinovic, Petar M.(2009) 'Applications of the ArgusLab4/AScore protocol in the structure-based binding affinity prediction of various inhibitors of group-1 and group-2 influenza virus neuraminidases (NAs)', Molecular Simulation, 35: 4, 311 — 324
To link to this Article: DOI: 10.1080/08927020802430752
URL: http://dx.doi.org/10.1080/08927020802430752

Molecular Simulation
Vol. 35, No. 4, April 2009, 311–324

Taylor & Francis
Taylor & Francis Group

Applications of the ArgusLab4/AScore protocol in the structure-based binding affinity prediction of various inhibitors of group-1 and group-2 influenza virus neuraminidases (NAs)

Marija L. Mihajlovic[ab] and Petar M. Mitrasinovic[b]*

[a]*Department of Physical Chemistry, University of Belgrade, Belgrade, Serbia;* [b]*Institute for Multidisciplinary Research, Belgrade, Serbia*

(*Received 4 May 2008; final version received 25 August 2008*)

Using the crystal structures of inhibitors bound to either group-2 or group-1 neuraminidases (NAs), AScore/ShapeDock (GaDock) scoring was shown to identify the binding modes in agreement with the experiment for all inhibitors docked in their own NA/inhibitor crystal structures. To investigate the effect of small changes in protein structure on predicted binding modes, in a set of 132 docking experiments (11 inhibitors docked in 12 group-2 NA structures), AScore/ShapeDock (GaDock) identified the correct binding modes of 116 complexes. In a total of 88 docking experiments (8 inhibitors docked in 11 group-1 NA structures), AScore/ShapeDock predicted 80 binding modes correctly. Flexible AScore/ShapeDock docking, as quite reproducible, is suggested to be convenient for designing novel H5N1 inhibitors.

Keywords: influenza virus neuraminidase; inhibitors; AScore; ArgusLab 4.0

1. Introduction

Two glycoproteins, haemagglutinin and neuraminidase, are contained in influenza virus membranes with their specific functions. While cell surface sialic acid receptor binding is mediated by haemagglutinin in order to trigger virus infection, neuraminidase removes sialic acid from virus and cellular glycoproteins after virus replication, thus facilitating virus release and the spread of infection to new cells [1]. Based on different antigenic properties of various glycoprotein molecules, influenza type A viruses are classified into the following subtypes: 16 for haemagglutinin (H1–H16) and 9 for neuraminidase (N1–N9) [2]. Two phylogenetically distinct groups, group 1 (N1, N4, N5, N8) and group 2 (N2, N3, N6, N7, N9), contain N1 and N2 neuraminidases (NAs) of viruses that currently circulate in humans [3]. One such virus, H5N1 avian influenza NA, is threatening a new pandemic [4,5]. Because vaccines are not yet available and a number of drugs are undergoing testing, infected patients are currently treated with two approved anti-influenza drugs, oseltamivir (Tamiflu) [6] and zanamivir (Relenza) [7] (Figure 1), targeting NA enzyme of virus. Due to reports on the virus resistance to the two approved drugs [8–11], the development of new anti-influenza molecules can be viewed as a priority [12]. Even though influenza virus NA is structurally well studied [13–17], the structure of H5N1 is particularly attractive because it offers new opportunities for drug design [18].

Computational methods are now a viable partner in experiments to design NA inhibitors [19]. A computational model of H5N1 neuraminidase has been reported recently, and the binding of H5N1 to commercial drugs has been consequently explored [20]. A similar modelling strategy has been employed to provide insights into the secret as to why H5N1 strains bear high resistance for the existing NA inhibitors [21]. The fact that several tens of different crystal structures of group-2 NAs are available in the Protein Data Bank (PDB) [22] has enabled extensive investigations of the effect of small changes in protein structure on predicted binding modes of known inhibitors by means of knowledge-based scoring functions [23]. There have also been indications that inhibitor structure–activity relationships do not apply across subtypes [24]. Taking into account these anomalies, the crystal structures of three group-1 NAs (N1, N4, N8) and their complexes with oseltamivir, zanamivir, DANA and peramivir have been determined [18]. Their active sites have also been compared with those of group-2 enzymes [18] against which the current drugs have been designed [14,25].

The ultimate goals of the docking and scoring technology applications at different stages of the drug discovery process are: (1) predicting the binding mode of a known active ligand, (2) identifying new ligands by means of virtual screening and (3) predicting the binding affinities of related compounds from a known active series [26]. Successful prediction of a ligand binding mode in a protein active site is the area where the most substantial progress has been achieved [27,28]. Docking studies, demonstrating that particular techniques can reproduce observed results in a published dataset, represent the first step for evaluating

*Corresponding author. Email: petar.mitrasinovic@cms.bg.ac.yu

ISSN 0892-7022 print/ISSN 1029-0435 online

DOI: 10.1080/08927020802430752
http://www.informaworld.com

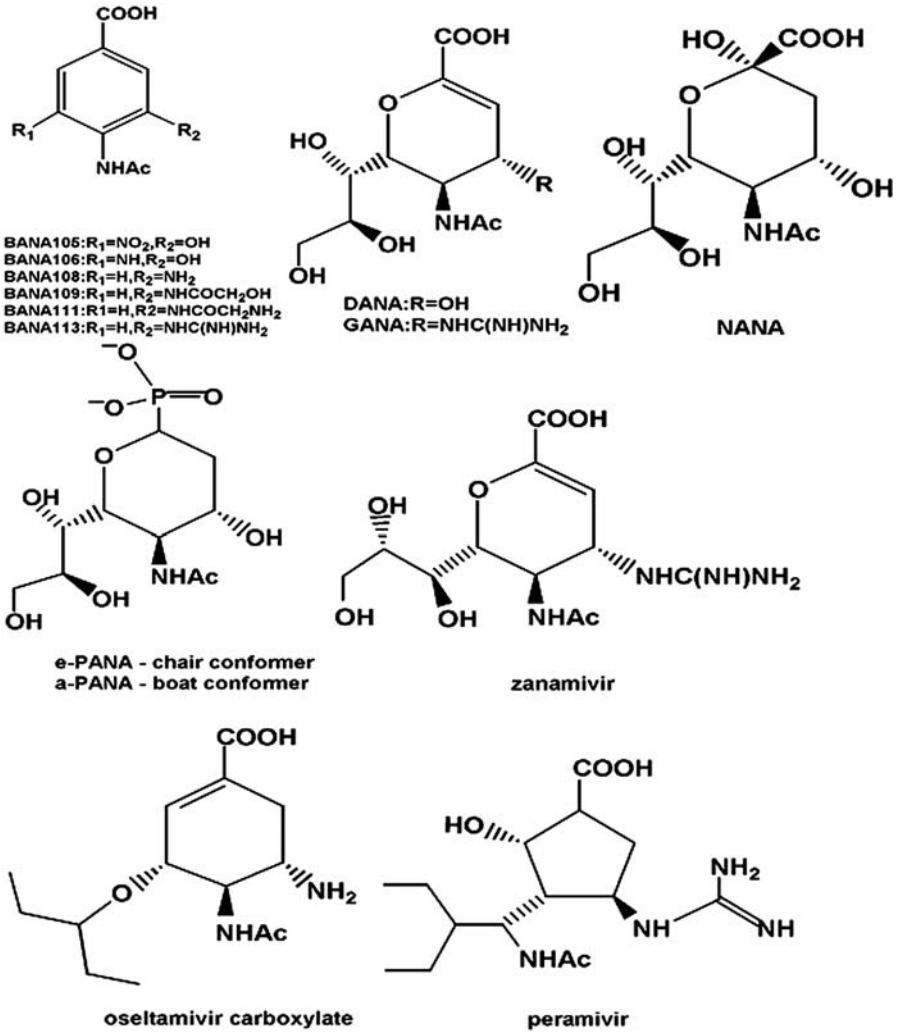

Figure 1. The chemical structures of influenza NA inhibitors.

the accuracy of newly developed or improved algorithms. As a consequence of the successful first step, the following step is based on prospective studies, particularly from industry where the opportunity for such work is the greatest [26]. In light of the previous results [23], the first objective of the present study is to explore the ability of ArgusLab 4.0, a recently introduced molecular modelling package in which molecular docking was implemented [29], to reproduce crystallographic binding orientations of various inhibitors bound to group-2 NAs, and to compare its accuracy with that of the QuantumLead program [30]. Since the structure of H5N1 suggests a wide spectrum of new opportunities for drug design in the context of a current pandemic threat by the worldwide spread of H5N1 avian influenza [18], the second objective is, herein, to estimate the accuracy of the same method to predict the binding modes of known inhibitors of group-1 NAs.

This article is outlined as follows. The theoretical background associated with AScore, an empirical scoring function, and with two distinct docking engines, ShapeDock and GaDock, is given in the 'Methodology' section. The theoretical section elucidates why the correct binding modes obtained by AScore with the ShapeDock algorithm are quite reproducible, while it is not always the case for the results obtained by AScore in combination with the GaDock search engine. Based on extensive calculations pertaining to the search for the best score of the binding orientations of various inhibitors relative to the substrates, the performance and efficiency of the ArgusLab 4.0 program are presented and discussed in the 'Results and discussion' section.

2. Methodology

2.1 Databases

The investigated structures are denoted throughout the paper by their PDB codes [22]. NA inhibitors contained by some of the PDB structures are shown in Figure 1.

The PDB IDs of group-2 NA structures are as follows: 1ivd, 1ivc, 1ive, 1ing, 1inh, 1inf, 2bat, 1ivf, 1nnc, 1inw, 1inx and 1ivg. The N2 A/Tokyo/3/67 subtypes are 1ivd (complex with guanidinobenzoic acid inhibitor, BANA105), 1ivc (with BANA106), 1ive (with BANA108), 1ing (with BANA109), 1inh (with BANA111), 2bat (with *N*-acetylneuraminic acid, NANA), 1ivf (with NeuAc2en, 2-deoxy-2,3-didehydro-*N*-acetylneuraminic acid, DANA), 1inx (with (4-acetamido-2,4-dideoxy-D-glycero-α-D-galacto-1-octopyranosyl) phosphonic acid, ePANA), 1inw (with (4-acetamido-2,4-dideoxy-D-glycero-D-galacto-β-octopyranosyl) phosphonic acid, aPANA) and 1ivg (no inhibitor). The N9 (Tern) subtype is 1nnc (with 4-guanidino-NeuAc2en, GANA), while the only one of type B/Lee/40 is 1inf (with BANA113).

The PDB IDs of group-1 NA structures are as follows: 2hty, 2hu0, 2hu4, 2ht5, 2htr, 2ht7, 2ht8, 2htq, 2htu, 2htv and 2htw. The N1 subtypes are 2hty (no inhibitor), 2hu0 (with oseltamivir, 20 μM) and 2hu4 (with oseltamivir, 0.5 mM), and the N8 subtypes are 2ht5 (no inhibitor), 2htr (with DANA), 2ht7 (with oseltamivir, 30-min soak), 2ht8 (with oseltamivir, 3-day soak), 2htq (with zanamivir) and 2htu (with peramivir). The N4 subtypes are 2htv (no inhibitor) and 2htw (with DANA).

2.2 *Molecular docking with ArgusLab 4.0*

The docking problem is conceivable as a complicated optimisation or an exhaustive search problem involving many degrees of freedom, and the development of efficient docking algorithms would be of vital importance for the design of new drugs. The ultimate goal is to find the optimal ligand/protein configurations, and accurately as well as consistently predict their binding free energy without relying on formal statistical mechanics approaches. To computationally accomplish the key objective within a reasonable time framework, an empirical scoring function (AScore) and two distinct docking engines (ShapeDock and GaDock) were developed in ArgusLab 4.0 [29].

2.2.1 *Fundamental idea behind empirical scoring*

Since a remarkable work of Böhm [31], a variety of scoring functions have appeared in the literature [32–40]. All of the approaches share the same assumption that the overall receptor–ligand binding free energy can be conceptually represented by a sum of some basic components

$$\Delta G_{\text{binding}} = \Delta G_{\text{motion}} + \Delta G_{\text{interaction}} + \Delta G_{\text{desolvation}} + \Delta G_{\text{configuration}}. \quad (1)$$

The separated terms account for the protein–ligand motion (ΔG_{motion}); the hydrogen bond, ionic, aromatic or lipophilic protein–ligand interaction ($\Delta G_{\text{interaction}}$); the desolvation-mediated protein–ligand binding ($\Delta G_{\text{desolvation}}$) and the binding free energy for a particular protein–ligand configuration ($\Delta G_{\text{configuration}}$), respectively. In contrast to force fields, empirical scoring functions are not derived from 'first principle'. Based on a set of protein–ligand complexes with experimentally determined structures and binding affinities, scoring functions are calibrated using multivariate regression analysis. The final form of a scoring function is affected by both the size and the quality of the training set. There are several principal features of various scoring approaches. Since they are derived from diverse protein–ligand complexes, their applications are not restricted to a particular series of ligands or a specific target receptor. Because each of the summing terms in an empirical scoring function is known to be important for the binding processes (Equation 1), it is associated with a clear physical meaning. Most importantly, a characteristic accuracy level of about 2 kcal/mol achieved in binding affinity predictions makes empirical scoring functions acceptable for the structure-based drug design purposes, such as virtual database screening and *de novo* ligand generation.

2.2.2 *The AScore scoring function*

The AScore [29] scoring function extends the previously reported XScore [39]. The total protein–ligand binding free energy is decomposed into several distinct components

$$\Delta G_{\text{binding}} = \Delta G_{\text{vdw}} + \Delta G_{\text{hydrophobic}} + \Delta G_{\text{H-bond}} + \Delta G_{\text{H-bond(chg)}} + \Delta G_{\text{deformation}} + \Delta G_0. \quad (2)$$

The dissected terms account for the van der Waals interaction between the ligand and the protein (ΔG_{vdw}), the hydrophobic effect ($\Delta G_{\text{hydrophobic}}$), the hydrogen bonding between the ligand and the protein ($\Delta G_{\text{H-bond}}$), the hydrogen bonding involving charged donor and/or acceptor groups ($\Delta G_{\text{H-bond(chg)}}$), the deformation effect ($\Delta G_{\text{deformation}}$) and the effects of the translational and rotational entropy loss in the binding process (ΔG_0), respectively. The separate $\Delta G_{\text{H-bond (chg)}}$ term (Equation 2) is the only addition to the XScore binding free energy of Wang and coworkers [39]. In contrast to XScore, the intra-ligand van der Waals energy is also included in the overall VDW term.

These contributions can be conveniently written as the following products: $\Delta G_{\text{vdw}} = C_{\text{vdw}} \cdot \text{VDW}$, $\Delta G_{\text{hydrophobic}} = C_{\text{hydrophobic}} \cdot \text{HP}$, $\Delta G_{\text{H-bond}} = C_{\text{H-bond}} \cdot \text{HB}$, $\Delta G_{\text{H-bond (chg)}} = C_{\text{H-bond (chg)}} \cdot \text{HB (chg)}$, $\Delta G_{\text{deformation}} = C_{\text{rotor}} \cdot \text{RT}$ and $\Delta G_0 = C_{\text{regression}}$. Each of the contributions possesses a specific regression coefficient multiplying a term that

has a physical meaning. Investigating the regression coefficients enables more profound insights into the receptor–ligand binding process. The physical definitions of the VDW, HP, HB and *RT* terms are given by the following four equations:

$$\mathrm{VDW} = \sum_{i}^{\text{ligand}} \sum_{j}^{\text{protein}} \left[\left(\frac{d_{ij,0}}{r_{ij}} \right)^{8} - 2 \left(\frac{d_{ij,0}}{r_{ij}} \right)^{4} \right] + \sum_{i}^{\text{ligand}} \sum_{j>i}^{\text{ligand}} \left[\left(\frac{d_{ij,0}}{r_{ij}} \right)^{8} - 2 \left(\frac{d_{ij,0}}{r_{ij}} \right)^{4} \right], \quad (3)$$

where $d_{ij,0}$ is the sum of the van der Waals radii of atoms i,j, while the intra-ligand *VDW* portion of this term excludes 1,2 and 1,3 bonded pairs.

$$\mathrm{HP} = \sum_{i}^{\text{ligand}} \sum_{j}^{\text{protein}} f(d_{ij}), \quad (4)$$

where the sum is over hydrophobic ligand–protein atom pairs and

$$f(d_{ij}) = \begin{cases} 1.0 \text{ for } d < d_{ij,0} + 0.5\,\text{Å} \\ 2/3 \cdot (d_0 + 2 - d) \text{ for } d_{ij,0} + 0.5\,\text{Å} < d \le d_{ij,0} + 2.0\,\text{Å} \\ 0 \text{ for } d > d_{ij,0} + 2.0\,\text{Å} \end{cases}$$

$$\mathrm{HB} = \sum_{i}^{\text{ligand}} \sum_{j}^{\text{protein}} \mathrm{HB}_{ij}, \quad (5)$$

where $\mathrm{HB}_{ij} = f(r_{ij})\ f(\theta_{1,ij})\ f(\theta_{2,ij})$, r_{ij} is the distance between donor/acceptor atoms, $\theta_{1,ij}$ is the angle between donor root–donor–acceptor and $\theta_{2,ij}$ is the angle between donor–acceptor–acceptor root. Each term in the sum varies between 1.0 and 0.0, depending on how close it is to the ideal value.

$$RT = \sum_{i}^{\text{ligand}} RT_i, \quad (6)$$

with $RT_i = 0$ if atom i is not involved in any torsion, $RT_i = 0.5$ if atom i is involved in one torsion, $RT_i = 1.0$ if atom i is involved in two torsions and $RT_i = 0.5$ if atom i is involved in more than two torsions.

2.2.3 *The ShapeDock and GaDock docking engines*

The ShapeDock docking engine approximates a complicated search problem. Flexible ligand docking is available by describing the ligand as a torsion tree. Groups of bonded atoms that do not have rotatable bonds are nodes, while torsions are connections between the nodes. Topology of the torsion tree is a determinative factor influencing efficient docking. A balanced tree with a large central node is presumably the favourite case. Two grids, overlaying the binding site, distinguish grid points with respect to the free volume of binding site. Fine grid is used to examine whether atoms of a pose fragment are inside or outside the binding site, while coarse grid is used to establish the search points inside the binding site. A set of energetically favourable rotations is generated by placing the root node of a ligand on a search point in the binding site. The torsion search of poses is defined by constructing torsions in breadth-first order for each rotation. Of the survived poses candidates, the *N* lowest energy poses (*N* is usually 50–150) makes the final set of poses undergoing coarse minimisation, reclustering and ranking. The AScore/ShapeDock docking protocol is fast, reproducible and formally explores all energy minima. To illustrate this standpoint, typical ShapeDock times for ligands with 10–15 torsions are shorter than 30 s on a 2.4 GHz Pentium computer.

The GaDock search engine employs the Lamarckian genetic algorithm to explore conformational flexibility of the ligand. This method applies a Lamarckian model of genetics, in which environmental adaptations of an individual's phenotype are reversely transcribed into its genotype and become heritable traits [41]. Because of the stochastic nature of this algorithm, it is difficult to define a convergence criterion. Consequently, the search procedure can easily get caught in a local minimum. Therefore, the AScore/GaDock docking protocol is robust, slow and inadequate to be easily reproducible.

3. Results and discussion

In this section, the efficiency of the ArgusLab4/AScore approach, in combination with the ShapeDock and GaDock search engines, respectively, is examined for known inhibitors bound to group-2 NAs. A correlation of these results with those obtained by the QuantumLead program is also expressed quantitatively using Pearson's correlation coefficient (r) approach. Consequently, the ArgusLab4/AScore/ShapeDock binding modes of group-1 NA inhibitors are explored.

3.1 The binding affinities of group-2 NA inhibitors: AScore/ShapeDock

To compare the binding sites of docked inhibitors in their highest ranked binding modes, root mean square deviations (RMSDs) of overlaid Cα and backbone atoms relative to 1ing are given in Table 1. The RMSD ranges for these overlays are between 0.26 and 0.45 Å for all Cα atoms and between 0.47 and 0.56 Å for backbone atoms. The RMSD range between 0.35 and 0.52 Å, which was

Table 1. Root mean square deviations (RMSDs) of overlaid Cα and backbone atoms in the binding sites and of docked group-2 NA inhibitors in their top-ranked binding mode using AScore/ShapeDock.

PDB ID	Inhibitor	Log IC_{50}[a]	RMSD[b] (Å)	RMSD[c] (Å)	RMSD[d] (Å)	<RMSD>[e] (Å)
1ivd	BANA105	−3.1	0.34	0.49	2.28	4.33
1ivc	BANA106	−1.7	0.26	0.46	1.01	1.72
1ive	BANA108	−1.7	0.32	0.46	1.58	2.47
1ing	BANA109	−2.4	–	–	0.74	1.49
1inh	BANA111	−2.3	0.32	0.53	1.81	1.42
1inf	BANA113	−5.0	0.45	0.56	1.04	1.47
2bat	NANA	−2.7	0.31	0.47	1.10	1.40
1ivf	DANA	−4.8	0.31	0.51	1.80	1.84
1nnc	GANA	−9.0	0.40	0.54	1.25	1.57
1inw	aPANA	−2.7	0.31	0.48	2.28	1.79
1inx	ePANA	−3.7	0.32	0.48	1.89	2.07
1ivg	None	–	0.32	0.49	–	–
Average			0.33	0.50	1.53	1.96

[a] Experimental values of IC_{50} for all BANAs were taken from [15]; for NANA, DANA and GANA from [17] and for aPANA and ePANA from [16]. [b] RMSD of Cα atoms in the binding site after overlay. The reference structure is 1ing. [c] RMSD of backbone atoms in the binding site relative to 1ing. [d] RMSD of the highest ranked binding mode of the inhibitor docked into its crystal structure. [e] Average RMSD of the highest ranked binding mode of the inhibitor over all 12 crystal structures.

previously reported for all Cα atoms of residues with heavy atoms closer than 5 Å to BANA109 in 1ing, as well as all Cζ atoms of the arginine residues [23(a)], is correctly between these two for Cα and backbone atoms (Table 1).

Figure 2 shows the AScore scoring results for the 11 inhibitors in their own crystal structures. The correlation ($r = 0.74$; Figure 2(a)) with the experiment improves to an r of 0.77 if ePANA is removed (Figure 2(b)), but if two

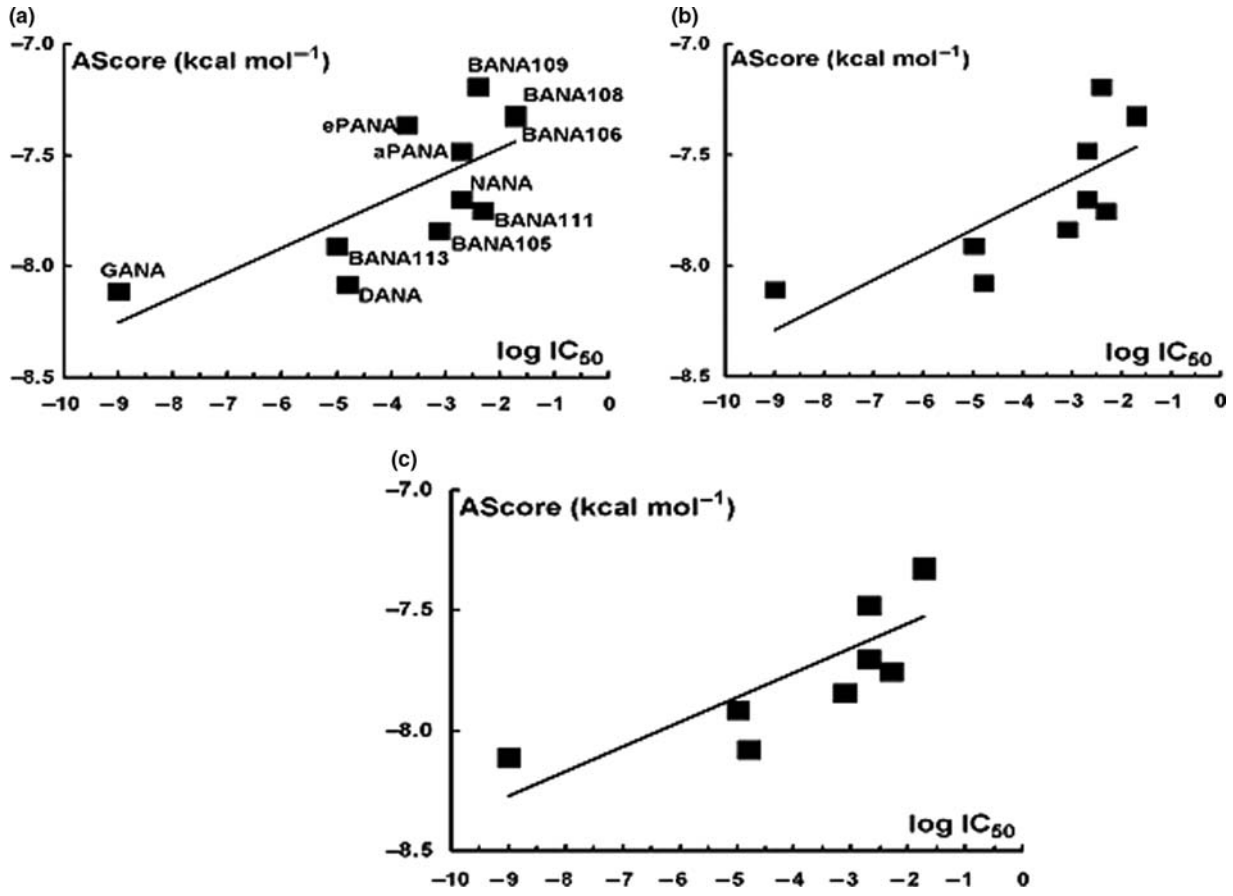

Figure 2. Correlation of the predicted AScore/ShapeDock binding affinities with measured ones for 11 (**a**, $r = 0.74$), 10 (**b**, ePANA removed, $r = 0.77$) and 9 (**c**, ePANA and BANA109 removed, $r = 0.80$) protein–ligand complexes of NA.

outliers (BANA109 and ePANA) are removed, the correlation improves to an r of 0.80 (Figure 2(c)). In accordance with the experiment, GANA was predicted to be the best binder (Figure 2(a)). The resulting overlay of 12 NA protein structures with docked GANAs is shown schematically in Figure 3.

Since RMSD of the top-ranked binding mode of each inhibitor docked into its crystal structure is below 2.5 Å (Table 1), all the inhibitors could thus be docked correctly into their crystal structures. To explore the sensitivity of the docking protocol to changes in the substrate structure, all 11 inhibitors were docked in all 12 NA crystal structures, and computed RMSDs are given in Table 2. Eighty-eight percent (70%) of the docked complexes is associated with RMSD between the docked and crystallographic binding modes of less than 2.5 (2.0) Å. This percentage is higher than that of the 82% (64%) previously reported [23(a)]. Besides, RMSD for each inhibitor averaged over all crystal structures is given in the last column of Table 1. With the exception of BANA105, the average RMSD of each ligand over all crystal structures is below 2.5 Å in the highest ranked binding mode (Table 1). The average RMSD for all inhibitors docked into the same crystal structure is shown on the

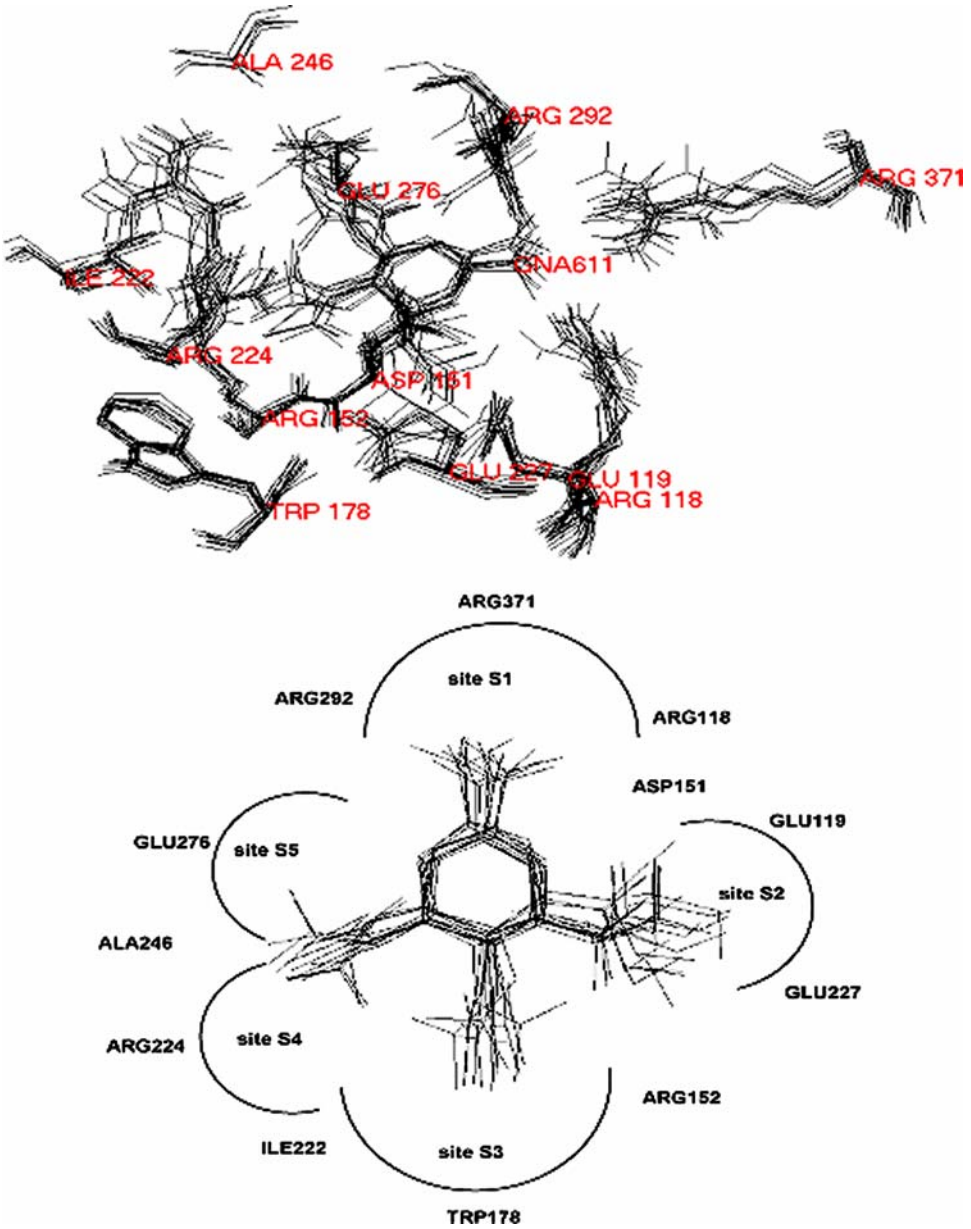

Figure 3. Overlay of 12 group-2 NA protein structures and GANA (denoted by GNA611) inhibitors (top). Overlay of GANA inhibitors with the general locations of important nearby residues (bottom). AScore/ShapeDock.

Table 2. RMSDs (in Å) of group-2 NA inhibitors docked in their highest ranked binding mode using AScore/ShapeDock.

Inhibitor	1ivd	1ivc	1ive	1ing	1inh	1inf	2bat	1ivf	1nnc	1inw	1inx	1ivg
BANA105	2.28	2.11	2.49	5.76	5.79	2.22	6.05	6.08	6.12	1.33	6.05	5.70
BANA106	1.11	1.01	2.46	0.57	2.82	2.18	0.47	2.85	1.19	1.47	1.47	2.98
BANA108	2.34	2.74	1.58	2.62	3.72	2.34	2.49	3.08	1.37	2.31	3.75	1.34
BANA109	1.38	1.84	1.96	0.74	1.34	1.52	1.05	1.55	1.88	1.65	1.66	1.26
BANA111	1.24	1.58	1.16	0.89	1.81	1.24	1.25	1.82	1.65	1.38	1.35	1.70
BANA113	1.59	1.89	0.46	1.04	1.69	1.04	1.97	1.16	1.82	1.41	1.99	1.58
NANA	1.47	1.85	1.66	1.34	1.73	1.32	1.10	1.25	0.81	1.31	1.39	1.60
DANA	2.09	2.65	2.15	2.19	2.24	2.28	0.74	1.80	0.97	1.66	2.25	1.12
GANA	1.90	1.84	1.00	1.51	1.27	2.06	1.67	1.55	1.25	1.15	2.22	1.37
aPANA	1.77	2.10	2.27	1.26	2.37	1.96	1.58	1.32	1.28	2.28	2.06	1.18
ePANA	2.25	1.74	1.78	1.85	2.74	2.25	2.15	2.26	2.03	1.84	1.89	2.07
Average	1.76	1.94	1.73	1.80	2.50	1.86	1.86	2.25	1.85	1.62	2.37	1.99

bottom line of Table 2. All the inhibitors could be docked correctly into 4 (1ivd, 1ive, 1inf and 1inw) of the 12 crystal structures, and for 9 structures the average RMSD of the docked inhibitors is below 2.0 Å (Table 2). In contrast to this observation, it was previously shown that all the inhibitors could be docked correctly into 2 of the 12 protein structures, and for 5 structures the average RMSD of the docked inhibitors was found to be less than 2.0 Å [23(a)]. Although some poses exhibit a low RMSD value (below 2.0 Å), it does not mean that they must exhibit the correct binding pattern and vice versa. Hence, to further assess the validity of the docking approach, the binding modes/orientations are analysed.

The highest ranked binding modes of the NA inhibitors docked in their own crystal structures are depicted in Figure 4. Note that the NH_2 group position of BANA108 was predicted accurately (Figure 4), in contrast to that previously placed in an incorrect pocket [23(a)]. The *N*-acetyl group locations (Figure 4) were identified much more accurately than those reported earlier [23(a)]. A key reason for it was the previous neglect of a water molecule mediating the interaction between the *N*-acetyl group and the NA protein (Figure 5). An unexpected binding orientation of the guanidinobenzoic acid inhibitor BANA113 in its crystal structure (PDB ID: 1inf) was very puzzled, because the guanidino group was established

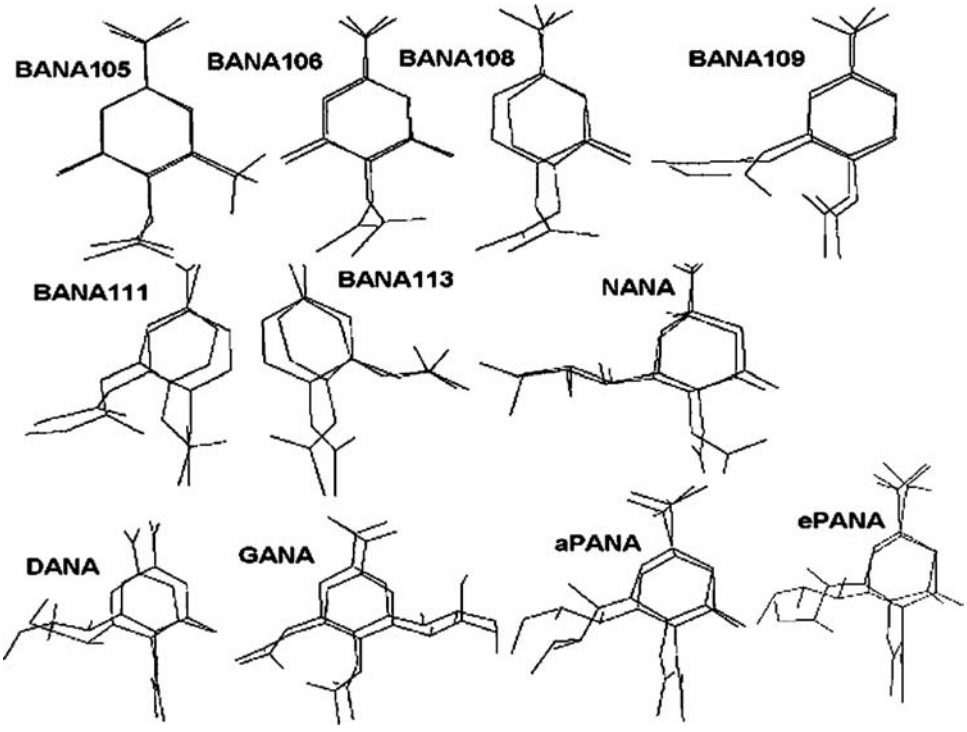

Figure 4. Superposition of crystallographic and the highest ranked binding modes of group-2 NA inhibitors. AScore/ShapeDock.

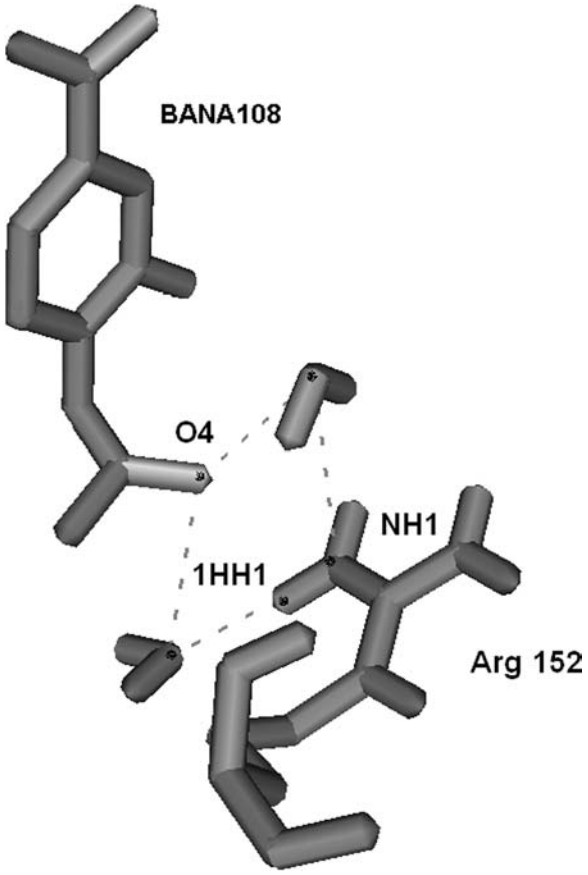

Figure 5. The water molecule-mediated interaction between the *N*-acetyl group in BANA108 and the NA protein.

to bind to a different pocket than that of GANA [17]. BANA113 was indeed rotated by 180° relative to GANA, thus enabling the *N*-acetyl and carboxylate groups to make the same interactions with the NA protein as GANA. The sudden flips in the orientation of inhibitors are presumably unique for charged and highly polar pockets [15,17]. Having two similar inhibitors with guanidino groups placed in different pockets was treated as a good example of investigating the robustness of a docking approach [36,37]. Table 2 shows that BANA113 was docked correctly in all of the 12 protein structures, while it was previously docked correctly in 8 of the 12 NA crystal structures [23(a)]. Noteworthy is GANA docked correctly in all of the 12 crystal structures (Table 2), while it could not be previously docked correctly in 7 of the 12 protein structures [23(a)]. Therefore, a preference for the guanidino group of GANA to be placed in an incorrect pocket containing Glu275 rather than in a correct one in the proximity of Glu117 and Glu226 [42] is not supported herein.

Based on the results presented by now, the AScore/ShapeDock approach, as a very consistent and reproducible algorithm, substantially outperforms the PMF score/docking approach. In contrast to AScore scoring, taking into account the separate contributions of the protein–ligand and intra-ligand van der Waals interactions, as well as the hydrogen bonding involving charged donor and/or acceptor groups [29], PMF scoring, rooted in the sum over all protein–ligand atom pair potentials as a function of the atom pair distance [36,37], underestimates electrostatic contributions to a great extent.

3.2 The binding affinities of group-2 NA inhibitors: AScore/GaDock

Table 3 displays that the RMSD of the top-ranked binding mode of each inhibitor docked into its crystal structure is below 2.5 Å, thus showing that all the inhibitors could be docked correctly into their crystal structures. The correlation ($r = 0.65$; Figure 6(a)) with the experiment improves to an r of 0.79 by removing BANA113 (Figure 6(b)), while the correlation gets substantially better by removing BANA108 and BANA113 ($r = 0.89$; Figure 6(c)). Since the AScore/GaDock highest ranked binding modes of all inhibitors, when superimposed on their own crystal structures, are quite similar to those given in Figure 4, they are not shown due to insufficient space in the present paper. In agreement with the experiment, GANA was predicted to be the best binder (Figure 6(a)).

To investigate the impact of small changes in substrate structure on the docking results, all 11 inhibitors were docked in all 12 NA crystal structures. Table 4 illustrates that 116 of the 132 protein–ligand complexes (88%) are associated with RMSDs between the docked and crystallographic binding modes of less than 2.5 Å, while RMSDs for 95 of a total of 132 docked structures (72%) are below

Table 3. Root mean square deviations (RMSDs) of docked group-2 NA inhibitors in their top-ranked binding mode using AScore/GaDock.

PDB ID	Inhibitor	Log IC_{50}[a]	RMSD[b] (Å)	RMSD[c] (Å)
1ivd	BANA105	−3.1	1.80	3.73
1ivc	BANA106	−1.7	1.93	2.24
1ive	BANA108	−1.7	2.42	2.78
1ing	BANA109	−2.4	1.51	1.04
1inh	BANA111	−2.3	1.66	1.50
1inf	BANA113	−5.0	1.84	1.40
2bat	NANA	−2.7	1.97	1.50
1ivf	DANA	−4.8	1.50	1.37
1nnc	GANA	−9.0	1.30	1.47
1inw	aPANA	−2.7	2.31	1.96
1inx	ePANA	−3.7	1.99	1.98
Average			1.84	1.91

[a] Experimental values of IC_{50} for all BANAs were taken from [15]; for NANA, DANA and GANA from [17] and for aPANA and ePANA from [16]. [b] RMSD of the highest ranked binding mode of the inhibitor docked into its crystal structure. [c] Average RMSD of the highest ranked binding mode of the inhibitor over all 12 crystal structures.

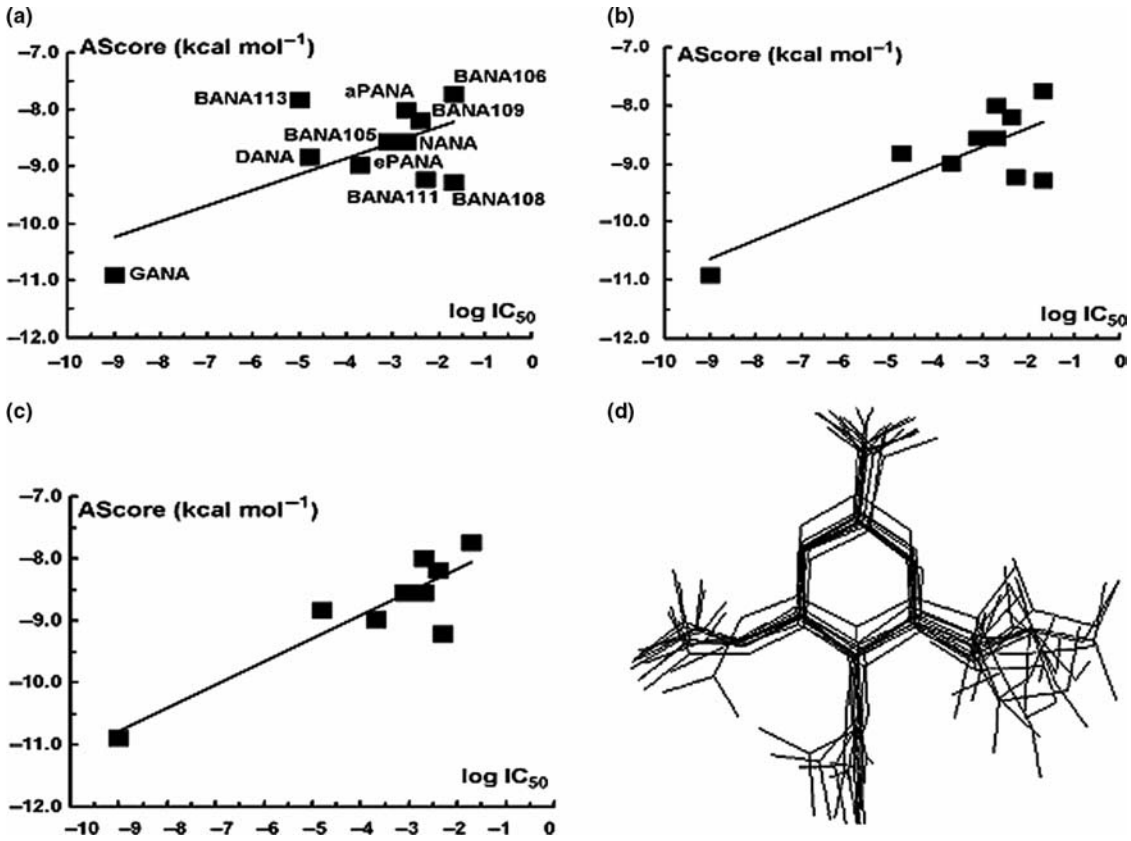

Figure 6. Correlation of the predicted AScore/GaDock binding affinities with measured ones for 11 (**a**, $r = 0.65$), 10 (**b**, BANA113 removed, $r = 0.79$) and 9 (**c**, BANA108 and BANA113 removed, $r = 0.89$) protein–ligand complexes of NA. The resulting overlay (**d**) of GANAs docked in all 12 protein structures given in Table 4.

2.0 Å. With the exception of BANA105 and BANA108, the average RMSD of each ligand over all crystal structures is below 2.5 Å in the highest ranked binding mode (Table 3). Table 4 shows that BANA113 was docked correctly in all of the 12 protein structures, while it was previously docked correctly in 8 of the 12 NA crystal structures [23(a)]. GANA was also docked correctly in all of the 12 crystal structures (Table 4), while it could not be previously docked correctly in 7 of the 12 protein structures [23(a)]. The overlay of GANAs docked in the 12 NA crystal structures is shown schematically in Figure 6(d). The guanidino group of GANA is thus shown to prefer to be placed in a correct pocket nearby Glu117 and Glu226 [42]. All the inhibitors could be docked correctly into 3 (1ivc, 2bat and 1ivf) of the 12 crystal structures, and for 8 structures the average RMSD of the docked inhibitors is

Table 4. RMSDs (in Å) of group-2 NA inhibitors docked in their highest ranked binding mode using AScore/GaDock.

Inhibitor	1ivd	1ivc	1ive	1ing	1inh	1inf	2bat	1ivf	1nnc	1inw	1inx	1ivg
BANA105	1.80	2.27	4.79	1.31	6.19	5.94	1.32	2.02	5.92	5.92	1.71	5.59
BANA106	2.59	1.93	2.91	2.77	1.69	2.33	0.77	1.59	2.61	2.87	2.54	2.33
BANA108	2.04	2.47	2.42	2.38	3.48	2.35	2.25	1.85	2.33	2.83	5.87	3.07
BANA109	0.97	1.26	1.13	1.51	0.86	1.15	0.92	0.60	0.95	1.04	0.63	1.44
BANA111	1.42	1.94	1.85	1.68	1.66	1.87	1.35	1.20	1.29	1.25	1.37	1.15
BANA113	0.59	0.76	1.95	1.16	0.99	1.84	1.66	1.85	0.91	1.89	1.46	1.68
NANA	1.59	1.56	1.75	0.76	1.84	1.39	1.97	1.39	1.39	1.54	1.35	1.43
DANA	0.59	0.98	1.23	1.25	1.24	1.56	1.98	1.50	1.67	0.63	1.53	2.25
GANA	1.42	1.36	1.85	2.04	1.19	1.39	1.36	1.17	1.30	1.50	1.24	1.81
aPANA	1.70	1.83	1.42	2.08	1.90	2.03	1.96	1.94	2.43	2.31	2.19	1.76
ePANA	2.14	1.91	2.40	2.11	1.92	1.78	1.80	1.82	1.71	2.20	1.99	1.99
Average	1.53	1.66	2.15	1.73	2.09	2.15	1.58	1.54	2.05	2.18	1.99	2.23

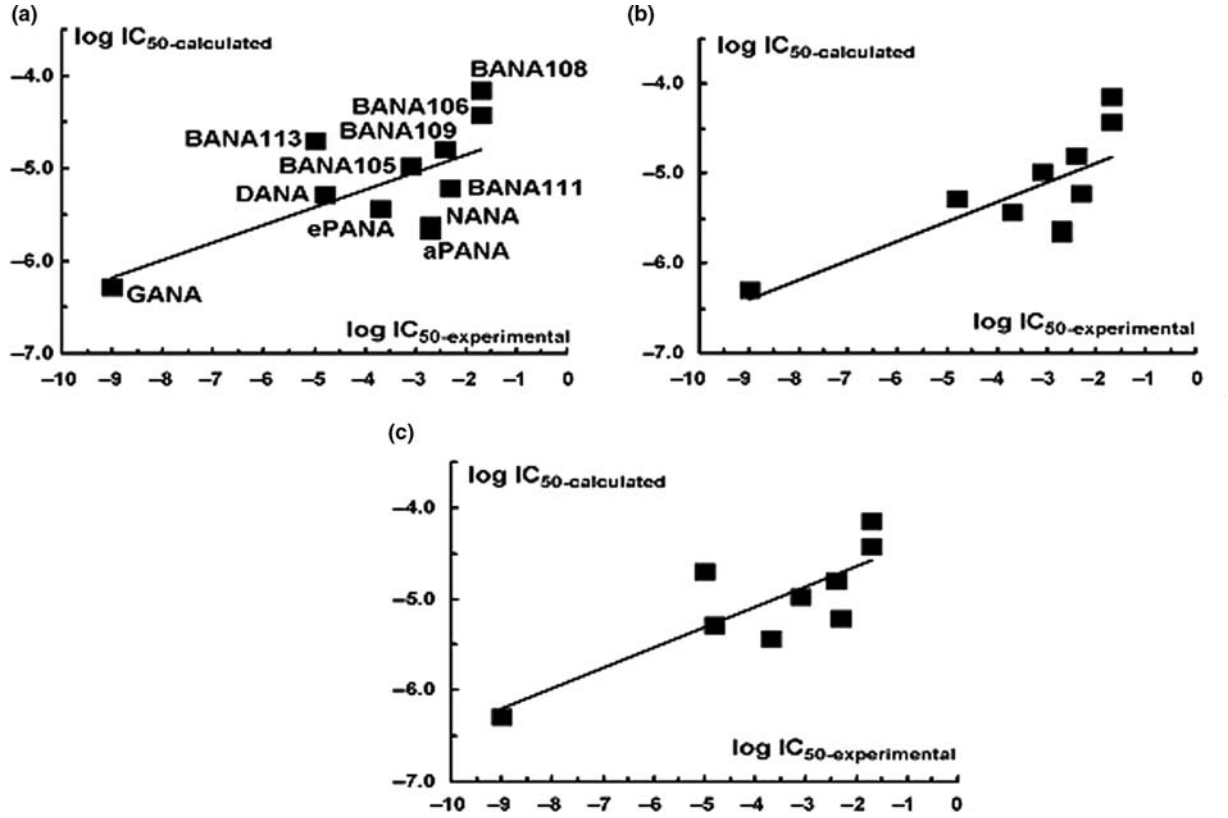

Figure 7. Correlation of the QuantumLead binding affinities with experimental ones for 11 (**a**, $r = 0.65$), 10 (**b**, BANA113 removed, $r = 0.75$) and 9 (**c**, NANA and aPANA removed, $r = 0.82$) protein–ligand complexes of NA.

below or about 2.0 Å (Table 4). Regardless of the difficulties associated with the stochastic nature of GaDock discussed in the previous section, its satisfactory performance is indicative in this particular situation.

3.3 Comparison between the ArgusLab and QuantumLead programs for group-2 NA inhibitors

To investigate the quality of the above-presented docking results obtained by ArgusLab 4.0 [29], the binding affinities of all 11 inhibitors docked in their own NA crystal structures were determined using QuantumLead [30]. Figure 7 shows the correlation of IC_{50} calculated by QuantumLead with experimental IC_{50}. In agreement with the experiment, GANA was predicted to be the best binder (Figure 7(a)). The correlation ($r = 0.65$; Figure 7(a)) with the experiment improves to an r of 0.75 by removing BANA113 (Figure 7(b)), while it further improves to an r of 0.82 by removing NANA and aPANA (Figure 7(c)). The initial correlation ($r = 0.65$) between predicted and measured binding affinities for the 11 protein–ligand complexes is the same as that given in Figure 6(a) for ArgusLab/AScore/GaDock. Also, an r of 0.74 given in Figure 2(a) for ArgusLab/AScore/ShapeDock clearly shows a better correlation than that ($r = 0.65$; Figure 7(a)) accomplished by QuantumLead. This quite satisfactory agreement of the ArgusLab-based results with those generated by QuantumLead is rooted in the composition of the QuantumLead binding free energy [30]. The free energy of non-covalent binding includes the hydrophobic and polar contributions, in addition to other two separate components corresponding to the rotational–translational entropy and the suppression of rotamer degrees of freedom, respectively [31,35].

3.4 The binding affinities of group-1 NA inhibitors: AScore/ShapeDock

Since the ArgusLab/AScore/ShapeDock protocol was established as a consistent and easily reproducible algorithm for group-2 NA inhibitors, we employed it to predict the binding affinities of various group-1 NA inhibitors. Table 5 shows RMSDs of overlaid Cα and backbone atoms in the protein active sites relative to 2htu. The RMSD ranges for these superpositions are between 0.22 and 0.66 Å for all Cα atoms, and between 0.25 and 0.79 Å for backbone atoms, thus being in agreement with those previously estimated for group-1 NA binding sites [18]. As peramivir was predicted to be the best binder, the resulting overlay of 11 NA

Table 5. RMSDs (in Å) of overlaid Cα and backbone atoms in the binding sites and of docked group-1 NA inhibitors in their highest ranked binding mode using AScore/ShapeDock.

PDB ID	Inhibitor	Log IC_{50}[a]	RMSD[b]	RMSD[c]	RMSD[d]	< RMSD>[e]
2hty	–	–	0.53	0.62	–	–
2hu0	oseltamivir	−5.7	0.60	0.68	1.66	1.83
2hu4	oseltamivir	−5.4	0.24	0.27	0.92	1.69
2ht5	–	–	0.50	0.61	–	–
2htr	DANA	−5.8	0.22	0.25	1.37	1.75
2ht7	oseltamivir	−5.7	0.66	0.79	0.73	1.70
2ht8	oseltamivir	−5.8	0.29	0.33	1.04	1.68
2htq	zanamivir	−5.6	0.33	0.38	2.45	3.13
2htu	peramivir	−6.4	–	–	2.38	2.12
2htv	–	–	0.51	0.58	–	–
2htw	DANA	−4.7	0.43	0.63	1.41	1.56
Average			0.43	0.51	1.50	1.93

[a] Estimated value of IC_{50} (Mol/l) using the QuantumLead program [30] for the inhibitor in its crystal structure. [b] RMSD of Cα atoms in the binding site after overlay. The reference structure is 2htu. [c] RMSD of backbone atoms in the binding site relative to 2htu. [d] RMSD of the highest ranked binding mode of the inhibitor docked into its crystal structure. [e] Average RMSD of the highest ranked binding mode of the inhibitor over all 11 crystal structures.

protein structures with docked peramivir is given in Figure 8. In this particular situation, RMSDs of less than 2.5 Å for the highest ranked binding mode (Table 5) indicate the correct docking of each inhibitor into its crystal structure. The highest ranked binding modes/orientations are shown in Figure 9.

To find out how changes in protein structure affect the quality of docking results, 8 inhibitors were docked

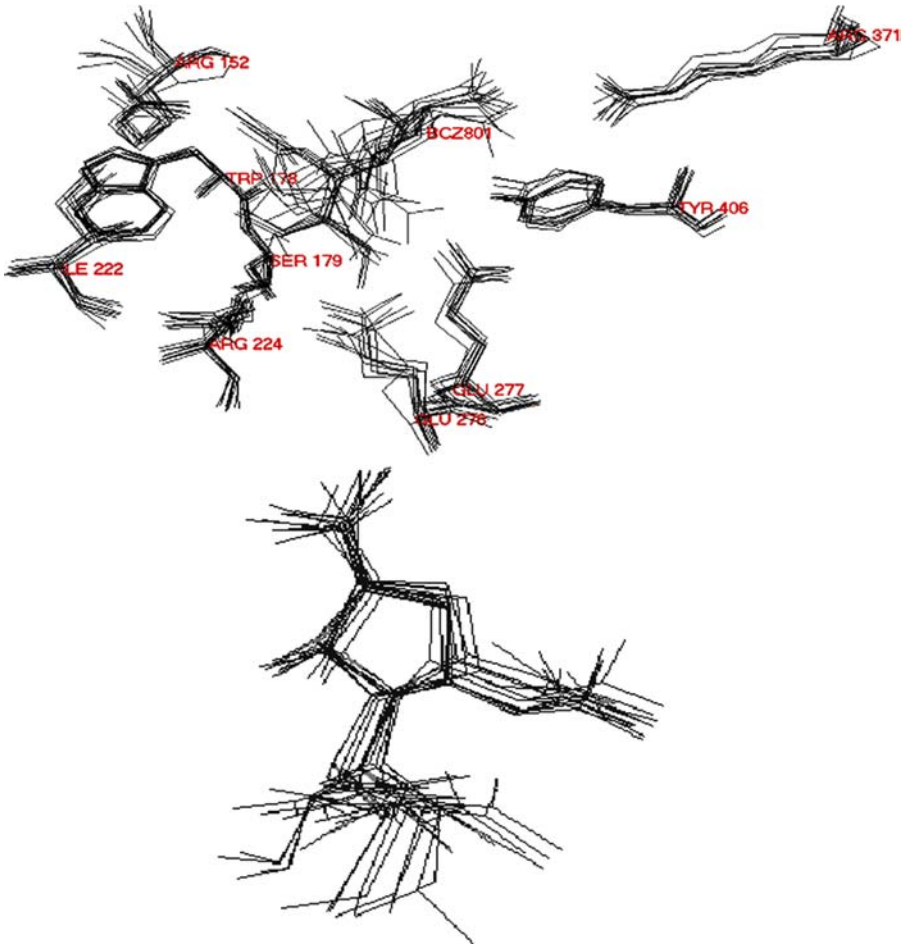

Figure 8. Overlay of 11 group-1 NA protein structures and peramivir (denoted by BCZ801) (top). Overlay of peramivir structures (bottom). AScore/ShapeDock.

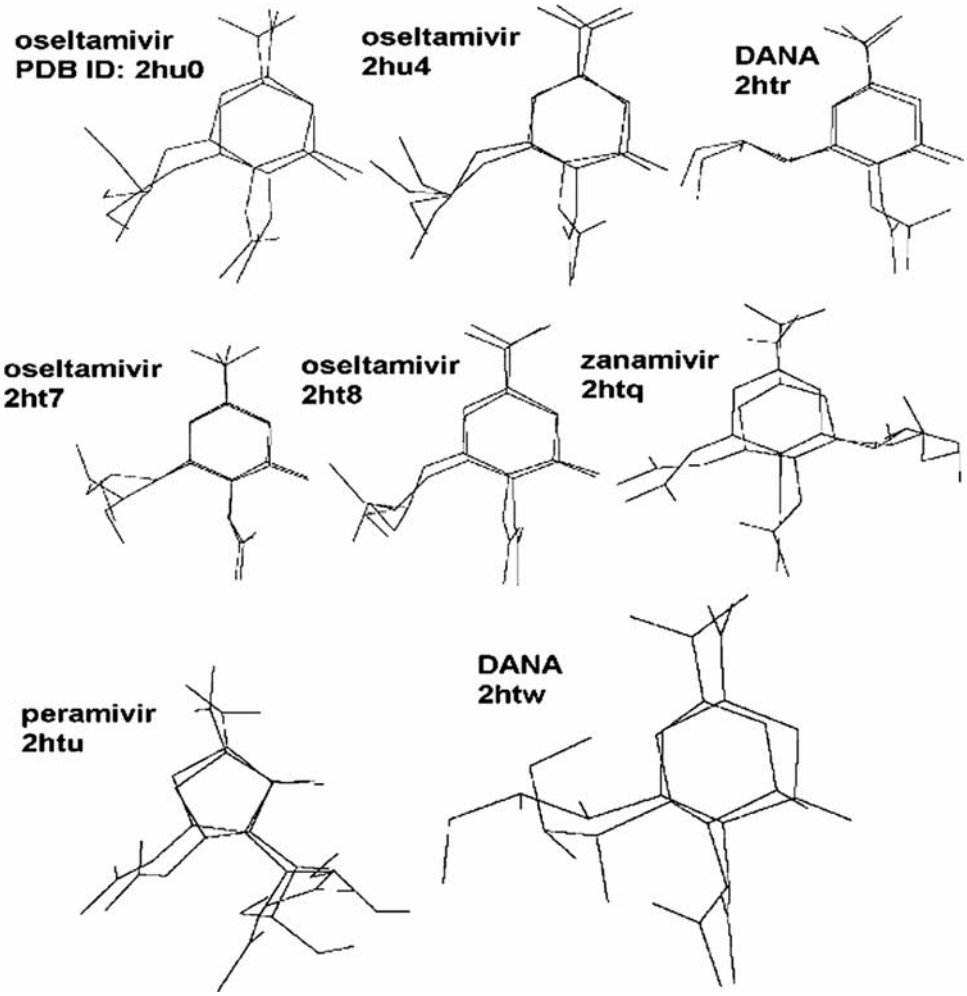

Figure 9. Superposition of crystallographic and the highest ranked binding modes of group-1 NA inhibitors. AScore/ShapeDock.

in 11 NA crystal structures. Of the 88 protein–ligand complexes (91%), 80 have RMSDs below 2.5 Å, while 59 of a total of 88 docked structures (67%) have RMSDs below 2.0 Å (Table 6). With the exception of zanamivir (PDB ID: 2htq), the average RMSD of each ligand over all crystal structures is below 2.5 Å (Table 5). Moreover, for 8 NA structures, the average RMSD of the docked inhibitors is below or about 2.0 Å (Table 6).

3.5 The mixing of known activity inhibitors to a set of randomly selected molecules of similar physicochemical profile

While it is important to verify the correctness of the binding mode and the ranking of molecules of known activities, it is so important to validate the approach by conducting a small vHTS experiment by mixing the known activity molecules to a set of randomly selected molecules (Table 7).

Table 6. RMSDs (in Å) of group-1 NA inhibitors docked in their highest ranked binding mode using AScore/ShapeDock.

Inhibitor	2hty	2hu0	2hu4	2ht5	2htr	2ht7	2ht8	2htq	2htu	2htv	2htw
oseltamivir	1.18	1.66	2.12	2.15	1.57	1.66	1.91	2.47	1.83	1.72	1.83
oseltamivir	2.28	1.57	0.92	1.35	1.46	0.99	1.98	1.56	2.06	2.38	2.03
DANA	1.32	2.31	1.76	1.87	1.37	2.07	1.09	1.47	1.61	2.36	2.04
oseltamivir	1.85	1.42	1.60	1.84	1.86	0.73	1.09	1.60	2.08	2.40	2.22
oseltamivir	1.00	1.25	0.93	1.89	1.79	2.40	1.04	1.57	2.19	2.24	2.17
zanamivir	3.18	4.92	1.43	1.14	5.25	1.26	3.17	2.45	1.23	5.39	5.01
peramivir	1.18	2.16	2.48	1.70	1.36	2.40	2.82	2.50	2.38	1.37	2.97
DANA	1.64	2.43	1.37	1.87	1.45	2.19	0.98	1.47	1.64	0.69	1.41
Average	1.70	2.22	1.58	1.73	2.01	1.71	1.76	1.89	1.88	2.32	2.46

Table 7. The AScore/ShapeDock binding free energies (kcal mol^{-1}) of known activity inhibitors mixed to a set of randomly selected molecules of similar physicochemical profile.

Inhibitor	AScore
3B[c]	−6.68
6B[c]	−6.72
5A[c]	−6.90
Zanamivir[a]	−6.90
7A[c]	−6.98
BANA108[b]	−7.32
8C[c]	−7.36
Oseltamivir[a]	−7.41
10B[c]	−7.52
Oseltamivir[a]	−7.52
16B[c]	−7.84
Oseltamivir[a]	−7.87
11C[c]	−7.90
Oseltamivir[a]	−7.99
DANA[b]	−8.08
GANA[b]	−8.11
8A[c]	−8.14
12A[c]	−8.24
DANA[a]	−8.31
13B[c]	−8.34
Peramivir[a]	−8.39
DANA[a]	−9.12

[a] The chosen inhibitors of known activity are all group-1 NA inhibitors (Table 5). [b] The chosen inhibitors of known activity are three (DANA, GANA, BANA108) group-2 NA inhibitors (Table 1). [c] The randomly chosen molecules of similar physicochemical profile are the oseltamivir structure-based analogues (3B, 5A, 6B, 7A, 8A, 8C, 10B, 11C, 12A, 13B, 16B) that were previously reported [43].

The ranking of poses based on AScore speaks in favour of the ability of the AScore/ShapeDock approach to extract active molecules from inactive ones. This observation was confirmed by our more recent study [44].

4. Summary

For a published dataset of structures composed of various inhibitors docked in group-2 (N2, N9) NA structures, the ArgusLab4/AScore/ShapeDock protocol was shown to identify the binding modes in agreement with the experiment. The composition of the AScore scoring function is a key reason for these successful performances. In contrast to the PMF [36,37] and XScore [39] protein–ligand binding free energies, AScore takes into account the separate contributions of the protein–ligand and intra-ligand van der Waals interactions, as well as the hydrogen bonding involving charged donor and/or acceptor groups [29]. Besides, the docking results generated by the ArgusLab4/AScore/ShapeDock protocol were demonstrated to be in agreement with those obtained by QuantumLead [30]. It is important to note that the correct binding modes and affinities for the complexes of group-2 NAs obtained by ArgusLab4/AScore/ShapeDock were shown to be both very consistent and easily reproducible. Consequently, an excellent performance of the same docking protocol was established for various inhibitors docked in group-1 (N1, N4, N8) NA structures.

Due to a recent pandemic threat by the worldwide spread of H5N1 avian influenza, the World Health Organisation has shown its profound concern regarding the possibility of having the virus spread among humans. Reports on the virus resistance to two approved anti-influenza drugs, oseltamivir (Tamiflu) and zanamivir (Relenza), as well as the lack of adequate vaccine, have raised the urgent question of developing new antiviral drugs. In this context, the ArgusLab4/AScore/ShapeDock approach is believed to be a valuable means for the structure-based design of novel H5N1 inhibitors.

Acknowledgements

This work was supported by the grant no. 143016B from the Ministry of Science of the Republic of Serbia. The authors gratefully acknowledge the reviewers for their valuable comments.

References

[1] B.R. Murphy and R.G. Webster, in *Fields Virology*, D.B.N. Fields, M. Knipe, and P. Howley, eds., Lippincott-Raven, Philadelphia, 1996, pp. 1397–1445.
[2] World Health Organization, *A Revision of the system of nomenclature for influenza viruses: a WHO memorandum*, Bull. World Health Organ. 58 (1980), pp. 585–591.
[3] J.D. Thompson, D.G. Higgins, and T.J. Gibson, *Improved sensitivity of profile searches through the use of sequence weights and gap excision*, Comput. Appl. Biosci. 10 (1994), pp. 19–29.
[4] C. Bender, H. Hall, J. Huang, A. Klimov, N. Cox, A. Hay, V. Gregory, K. Cameron, W. Lim, and K. Subbarao, *Characterization of the surface proteins of influenza A (H5N1) viruses isolated from humans in 1997–1998*, Virology 254 (1999), pp. 115–123.
[5] World Health Organization, *Global influenza program surveillance network. Evolution of H5N1 avian influenza viruses in Asia*, Emerg. Infect. Dis. 11 (2005), pp. 1515–1521.
[6] C. Kim, W. Lew, M. Williams, H. Liu, L. Zhang, S. Swaminathan, N. Bischofberger, M. Chen, D. Mendel, and C. Tai, et al., *Influenza neuraminidase inhibitors possessing a novel hydrophobic interaction in the enzyme active site: design, synthesis, and structural analysis of carbocyclic sialic acid analogues with potent anti-influenza activity*, J. Am. Chem. Soc. 119 (1997), pp. 681–690.
[7] M. von Itzstein, W. Wu, M. Pegg, J. Dyason, B. Jin, T. Phan, M. Smythe, H. White, S. Oliver, P. Colman, et al., *Rational design of potent sialidase-based inhibitors of influenza virus replication*, Nature 363 (1993), pp. 418–423.
[8] A.C. Hurt, P. Selleck, N. Komadina, R. Shaw, L. Brown, and I.G. Barr, *Susceptibility of highly pathogenic A (H5N1) avian influenza viruses to the neuraminidase inhibitors and adamantanes*, Antiviral Res. 73 (2007), pp. 228–231.
[9] M. Baz, Y. Abed, and G. Boivin, *Characterization of drug-resistant recombinant influenza A/H1N1 viruses selected* in vitro *with peramivir and zanamivir*, Antiviral Res. 74 (2007), pp. 159–162.
[10] L. Gillim-Ross and K. Subbarao, *Can immunity induced by the human influenza virus N1 neuraminidase provide some protection from avian influenza H5N1 viruses?* PLOS Medicine 4 (2007), pp. 226–228.
[11] M.A. Rameix-Welti, F. Agou, P. Buchy, S. Mardy, J. Aubin, M. Véron, S. van der Werf, and N. Naffakh, *Natural variation can significantly alter the sensitivity of influenza A (H5N1) viruses to oseltamivir*, Antimicrob. Agents Chemother 50 (2006), pp. 3809–3815.

[12] R.G. Webster, M. Peiris, H. Chen, and Y. Guan, *H5N1 outbreaks and enzootic influenza*, Infect. Dis. 12 (2006), pp. 3–8.
[13] J.N. Varghese and P.M. Colman, *Three-dimensional structure of the neuraminidase of influenza virus A/Tokyo/3/67 at 2·2 Å resolution*, J. Mol. Biol. 221 (1991), pp. 473–486.
[14] J.N. Varghese, W.G. Laver, and P.M. Colman, *Structure of the influenza virus glycoprotein antigen neuraminidase at 2.9 Å resolution*, Nature 303 (1983), pp. 35–40.
[15] S. Singh, M.J. Jedrzejas, G.M. Air, M. Luo, W.G. Laver, and W.J. Brouillette, *Structure-based inhibitors of influenza virus sialidase. A benzoic acid lead with novel interaction*, J. Med. Chem. 38 (1995), pp. 3217–3225.
[16] C.L. White, M.N. Janakiraman, W.G. Laver, C. Philippon, A. Vasella, G.M. Air, and M. Luo, *A sialic acid-derived phosphonate analog inhibits different strains of influenza virus neuraminidase with different efficiencies*, J. Mol. Biol. 245 (1995), pp. 623–634.
[17] E.A. Sudbeck, M.J. Jedrzejas, S. Singh, W.J. Brouillette, G.M. Air, W.G. Laver, Y.S. Babu, S. Bantia, P. Chand, N. Chu, et al., *Guanidinobenzoic acid inhibitors of influenza virus neuraminidase*, J. Mol. Biol. 267 (1997), pp. 584–594.
[18] R.J. Russell, L.F. Haire, D.J. Stevens, P.J. Collins, Y.P. Lin, G.M. Blackburn, A.J. Hay, S.J. Gamblin, and J.J. Skehel, *The structure of H5N1 avian influenza neuraminidase suggests new opportunities for drug design*, Nature 443 (2006), pp. 45–49.
[19] C. Sangma and S. Hannongbua, *Structural information and computational methods used in design of neuraminidase inhibitors*, Curr. Comput. Aided Drug Design 3 (2007), pp. 113–132.
[20] P. Nimmanpipug, J. Jitonnom, C. Ngaojampa, S. Hannongbua, and V.S. Lee, *A computational H5N1 neuraminidase model and its binding to commercial drugs*, Mol. Simul. 33 (2007), pp. 487–493.
[21] D-Q. Wei, Q-S. Du, H. Sun, and K-C. Chou, *Insights from modeling the 3D structure of H5N1 influenza virus neuraminidase and its binding interactions with ligands*, Biochem. Biophys. Res. Commun. 344 (2006), pp. 1048–1055.
[22] H.M. Berman, J. Westbrook, Z. Feng, G. Gilliland, T.N. Bhat, H. Weissig, I.N. Shindyalov, and P.E. Bourne, *The protein data bank*, Nucleic Acids Res. 28 (2000), pp. 235–242.
[23] (a) I. Muegge, *The effects of small changes in protein structure on predicted binding modes of known inhibitors of influenza virus neuraminidase: PMF-Scoring in DOCK4*, Med. Chem. Res. 9 (1999), pp. 490–500; (b) A.M. Abu Hammada, F.U. Afifia, and M.O. Taha, *Combining docking, scoring and molecular field analyses to probe influenza neuraminidase-ligand interactions*, J. Mol. Graph. Model. 26 (2007), pp. 443–456; (c) L. Birch, C.W. Murray, M.J. Hartshorn, I.J. Tickle, and M.L. Verdonk, *Sensitivity of molecular docking to induced fit effects in influenza virus neuraminidase*, J. Comput. Aided Mol. Design 16 (2002), pp. 855–869; (d) C.W. Murray, C.A. Baxter, and A.D. Frenkel, *The sensitivity of the results of molecular docking to induced fit effects: application to thrombin, thermolysin and neuraminidase*, J. Comput. Aided Mol. Design 13 (1999), pp. 547–562; (e) M.R. Landon, R.E. Amaro, R. Baron, C.H. Ngan, D.Ozonoff, J.A. McCammon, and S. Vajda, *Novel druggable hot spots in avian influenza neuraminidase H5N1 revealed by computational solvent mapping of a reduced and representative receptor ensemble*, Chem. Biol. Drug. Des. 71 (2008) pp. 106–116.
[24] W.J. Brouillette, S. Bajpai, S. Ali, S. Velu, V. Atigadda, B. Lommer, J. Finley, M. Luo, and G. Air, *Pyrrolidinobenzoic acid inhibitors of influenza virus neuraminidase: modifications of essential pyrrolidinone ring substituents*, Bioorg. Med. Chem. 11 (2003), pp. 2739–2749.
[25] A.T. Baker, J.N. Varghese, W.G. Laver, G.M. Air, and P.M. Colman, *Threedimensional structure of neuraminidase of subtype N9 from an avian influenza virus*, Proteins 2 (1987), pp. 111–117.
[26] A.R. Leach, B.K. Shoichet, and C.E. Peishoff, *Prediction of protein–ligand interactions. Docking and scoring: successes and gaps*, J. Med. Chem. 49 (2006), pp. 5851–5852.
[27] E.M. Krovat, T. Steindl, and T. Langer, *Recent advances in docking and scoring*, Curr. Comput. Aided Drug Design 1 (2005), pp. 93–102.
[28] V. Mohan, A.C. Gibbs, M.D. Cummings, E.P. Jaeger, and R.L. DesJarlais, *Docking: successes and challenges*, Curr. Pharm. Design 11 (2005), pp. 323–333.
[29] M.A. Thompson, *ArgusLab 4.0.1*, Planaria Software LLC, Seattle, WA, http://www.arguslab.com
[30] QuantumLead 3.3.0, Quantum Pharmaceuticals, Moscow, http://q-pharm.com
[31] H.J. Böhm, *The development of a simple empirical scoring function to estimate the binding constant for a protein-ligand complex of known three-dimensional structure*, J. Comput. Aided Mol. Design 8 (1994), pp. 243–256.
[32] A.N. Jain, *Scoring noncovalent protein–ligand interactions: a continuous differentiable function tuned to compute binding affinities*, J. Comput. Aided Mol. Design 10 (1996), pp. 427–440.
[33] M.D. Eldridge, C.W. Murray, T.R. Auton, G.V. Paolini, and R.P. Mee, *Empirical scoring functions: I. The development of a fast empirical scoring function to estimate the binding affinity of ligands in receptor complexes*, J. Comput. Aided Mol. Design 11 (1997), pp. 425–445.
[34] R.D. Head, M.L. Smythe, T.I. Oprea, C.L. Waller, S.M. Green, and G.R. Marshall, *VALIDATE: a new method for the receptor-based prediction of binding affinities of novel ligands*, J. Am. Chem. Soc. 118 (1996), pp. 3959–3969.
[35] H.J. Böhm, *Prediction of binding constants of protein ligands: a fast method for the prioritization of hits obtained from de novo design or 3D database search programs*, J. Comput. Aided Mol. Design 12 (1998), p. 309.
[36] I. Muegge and Y.C. Martin, *A general and fast scoring function for protein-ligand interactions: a simplified potential approach*, J. Med. Chem. 42 (1999), pp. 791–804.
[37] I. Muegge, Y.C. Martin, P.J. Hajduk, and S.W. Fesik, *Evaluation of PMF scoring in docking weak ligands to the FK506 binding protein*, J. Med. Chem. 42 (1999), pp. 2498–2503.
[38] R. Wang, Y. Gao, and L. Lai, *SCORE: A new empirical method for estimating the binding affinity of a protein-ligand complex*, J. Mol. Model. 4 (1998), pp. 379–394.
[39] R. Wang, L. Lai, and S. Wang, *Further development and validation of empirical scoring functions for structure-based binding affinity prediction*, J. Comput. Aided Mol. Design 16 (2002), pp. 11–26.
[40] N. Moitessier, P. Englebienne, D. Lee, J. Lawandi, and C.R. Corbeil, *Towards the development of universal, fast and highly accurate docking/scoring methods: a long way to go*, British J. Pharmacol. 153 (2008), pp. S7–S26.
[41] G.M. Morris, D.S. Goodsell, R.S. Halliday, R. Huey, W.E. Hart, R.K. Belew, and A.J. Olson, *Automated docking using a Lamarckian genetic algorithm and an empirical binding free energy function*, J. Comp. Chem. 19 (1999), pp. 1639–1662.
[42] M.J. Jedrzejas, S. Singh, W.J. Brouillette, G.M. Air, and M. Luo, *A strategy for theoretical binding constant, Ki, calculations for neuraminidase aromatic inhibitors designed on the basis of the active site structure of influenza virus neuraminidase*, Proteins 23 (1995), pp. 264–277.
[43] Q-S. Du, S-Q. Wang, and K-C. Chou, *Analogue inhibitors by modifying oseltamivir based on the crystal neuraminidase structure for treating drug-resistant H5N1 virus*, Biochem. Biophys. Res. Commun. 362 (2007), pp. 525–531.
[44] M.L. Mihajlovic and P.M. Mitrasinovic, *Another look at the molecular mechanism of the resistance of H5N1 influenza A virus neuraminidase (NA) to oseltamivir (OTV)*, Biophys. Chem. 136 (2008), pp. 152–158.